Hydrogeochemical analysis and identification of weathering processes to determine the solute sources in meltwater of Chaturangi glacier, Garhwal Himalaya, India

Harish Bisht¹, Bahadur Kotlia¹, Kireet Kumar², Prakash Arya³, Saurabh Sah², Mohit Tiwari², and Rajeev Upadhyay¹

¹Kumaun University ²GB Pant National Institute of Himalayan Environment and Development ³Indian Institute of Science

September 11, 2020

Abstract

This paper presents an insight on the major ion chemistry of Chaturangi glacier meltwater and chemical weathering processes to identify ionic sources and factors controlling the ionic composition of meltwater during the ablation year 2015 and 2016. The analytical results show that the meltwater is slightly acidic in nature with Mg-HCO3 and Ca-HCO3 dominated hydrochemical facies in years 2015 and 2016 respectively. In glacier meltwater, Ca2+ is the most dominant cation and HCO3- is the most dominant anion in both the years. Due to less anthropogenic influence, chemical weathering of the surrounding rocks is the foremost mechanism, controlling the hydrogeochemistry of meltwater. The gibbs plot and mineralogy of surrounding rocks suggests that ionic concentration of meltwater is mainly controlled by rock weathering with little contribution from the atmosphere. A comparatively higher contribution of (Ca+Mg) in total cations and higher elemental ratio of (Ca+Mg)/(Na+K) (1.47 ± 0.14) and (1.44 ± 0.28) in year 2015 and 2016 respectively, clearly demonstrates that chemical composition is mainly controlled by carbonate weathering and partly by silicate weathering. Furthermore, the low elemental ratio of $(Na+K)/TZ-(0.41\pm0.02)$ and (0.22 ± 0.05) in 2015 and 2016 respectively also suggests that carbonate weathering is a dominant geochemical process controlling meltwater chemistry of the study area. In addition the ion denudation rate was also calculated for both the years. The results shows that cation denudation rate of meltwater of Chaturangi glacier were 32.84 and 22.30 ton/km2/ablation during 2015 and 2016 respectively, whereas the anion denudation rates were 205.43 and 170.24 ton/km2/ablation in 2015 and 2016 respectively.

1. Introduction

Generally, the Himalaya contains largest deposition of snow and glacier ice outside the polar region (Bolch et al., 2012; Kulkarni & Karyakarte, 2014) and this region has a total of 9,575 glaciers, covering an area of about 40,000 km² (Raina & Srivastava, 2008), and is aptly called as the "Water Tower of Asia" (Dyurgerov & Maier, 1997). The Himalayan glaciers are situated at an altitude above 3,500 m away from the settlement of human inhabitants (Thayyen, Gergan, & Dobhal, 2007). The eastern and central Himalayan glaciers receive moisture from the Indian Summer Monsoon (ISM), whereas western glaciers pick up the moisture from the Mid Latitude Westerlies or Indian Winter Monsoon (IWM) (Dimri, Yasunari, Kotlia, Mohanty, & Sikka, 2016; Sharma et al., 2016). Hydrogeochemical study of the meltwater drained from different glaciers is important because of increasing demand of freshwater for population living in the downstream regions (Bisht, Arya, & Kumar, 2018). Such a study also provides important information about geology of the area, material loads into the oceans, atmospheric precipitation and types of rock weathering (Xu, Hou, An, Liu, & Dong, 2010). The hydrogeochemical characterization of glacier meltwater varies for different glaciers, largely

due to different lithology (Collins, 1979; Ramanathan, 2011). Various solutes in the meltwater streams are mainly obtained from chemical weathering of different surrounding rocks including small contribution from atmospheric aerosols (Carling, Rupper, Fernandez, Tingey, & Harrison, 2017; Kumar et al., 2009; Tiwari et al., 2018) which in turn is mainly influenced by mainly by lithology, soil cover, rainfall, discharge, temperature and relief (Noh, Huh, Qin, & Ellis, 2009; Raymo & Ruddiman, 1992; Shin, Ryu, Park, & Lee, 2011).

The processes of chemical weathering are more intense in glaciated regions than the tropics (Souchez & Lemmens, 1987), the higher rate in the former is primarily due to long residence time of meltwater to the bedrock (Singh et al., 2012). Godsey, Kirchner and Clow (2009) and Clow and Mast (2010) suggested that chemical weathering of rock forming minerals provides solutes, which generally control the hydrochemistry of a stream. The higher concentration of HCO_3^- in glacier meltwater is an indicative of higher weathering of silicate-dominant lithology of the area, whereas the higher Cl^- ion may indicate the contribution of rainwater (Singh, Ramanathan, Pottakkal, & Kumar, 2014a). The glaciated regions are perfect environment to study rock-water interaction and their role in solute dynamics of glacier meltwater (Sah et al., 2017). In glacial environment, the chemical weathering of surrounding rocks is a primary source of concentration of ions in the meltwater. However, the secondary source of ions in glacier meltwater is atmospheric precipitation (Hallet, 1976). The dissolved ionic and elemental fluxes carried by streams are regulated by chemical weathering, whereas particulate transport is determined by physical weathering of rocks (Krishnaswami & Singh, 2005).

The hydrochemical studies of the Himalayan glaciers are less documented as compared to Arctic and Alpine glaciers, probably due to difficulty in data collection at higher altitudes (Singh et al., 2014a). However, some studies (e.g., Kumar et al., 2009; Singh et al., 2012; Singh et al., 2013; Singh et al., 2014a,b; Sah et al., 2017) have been dealt with the hydrochemistry of meltwater draining from Gangotri glacier and its tributaries but none of these have discussed in detail the hrdrogeochemical characteristics of tributary glaciers because of limited dataset and lack of seasonal sampling of meltwater. To fill this gap, we have attempted an integrated approach to investigate the major ion chemistry, ionic flux, detailed hydrogeochemical weathering processes and source identification of various ions in the meltwater draining from the Chaturangi glacier based on the entire ablation data from 2015 to 2016.

2. Study area and regional geology

The Chaturangi glacier (30° 54' 08"- 30deg 54' 28" N and 79deg 15' 19"- 79deg 6' 18" E), situated in the Uttarkashi district of Uttarakhand, India (Figure 1) is 21.1 km long east-west-flowing valley type glacier which occupies an area of about 43.83 km² (Bisht, Rani, Kumar, Sah, & Arya, 2019) with a catchment area of about 214.8 km² (Orr, Owen, Saha, & Caffee, 2019). It is the longest inactive tributary glacier (not connected to the main trunk) of the Gangotri glacier system, connected with the Gangotri glacier till 1971 (Vohra, 1988; Bisht et al., 2020b), band was detached from the main trunk after 1989 (Bisht et al., 2019). At present, the snout of the Chaturangi glacier (Figure 2a) is located at 4,380 m from where the meltwater stream (Chaturangi river) originates (Bisht et al., 2019). The shape of the glacier snout keeps changing due to splitting of ice blocks from the terminus and subsidence at glacier portal (Bisht et al., 2020a). The regional scale precipitation is mainly influenced by the ISM as well as IWM (Kumar et al., 2018). Presently, the glacier comprises more than three active (connected with the trunk) tributary glaciers (Suralaya, Seeta, Vashuki, etc.) which form a part of the Chaturangi glacier system. The ablation zone is partially covered by the sediment, transported by erosion of the valley walls on the glacier surface. In this zone, the transverse and longitudianal crevasses are present on the glacier surface (Figure 2b). The small glacial lakes were also observed on the surface of the glacier (Figure 2c).

Geologically, the study area falls above the Main Central Thrust (MCT). The rocks are composed of the Higher Himalaya crystalline sequence (HHC) and Lesser Himalayan sequence (LHS), comprising mainly of Vaikrita group of gneisses, Harsil (meta) sediments, tourmaline leucogranite, Bhairongathi granite and Martoli formation (meta) sediments (Figure 3). The granite is composed mainly of quartz, alkali feldspar, biotite, muscovite and also contain crystals of tourmaline. The gneiss of this area is intruded by the granite which forms granitic gneiss. The Jhala normal fault passes from the study area, separating quartzo-feldpathic sillimanite gneiss from Harsil metasedimentary rocks (Searle, Noble, Hurford, & Rex, 1999). The geomorphic

evolution of this region is due to the neotectonic activity (Bali, Awasthi, & Tewari, 2003), and the present landform is an integrated outcome of glacio-tectonic movements and weathering processes (Bisht et al., 2020a).

3. Methodology

Sample collection

The glacier meltwater sampling site was selected about 0.5 km downstream from the present position of snout (Figure 1). A total of 118 samples in year 2015 and 122 samples in year 2016 were collected in 500 ml prewashed plastic bottles during both the ablation (June to September) seasons. The samples were collected according to the method given by Ostrem (1975) and the sample bottles were tightly closed and placed in a dark location to avoid changes resulting from the exposure to sunlight. All collected samples were carried to the Water Processing and Management (WPM) laboratory of G. B. Pant National Institute of Himalayan Environment and Sustainable Development Kosi-Katarmal Almora, Uttarakhand. In addition, fresh rock samples were also collected from the catchment of the Chaturangi glacier to identify the mineral assemblages which contributing ions into the glacier melt.

Onsite measurements

Onsite analysis of potential of hydrogen (pH), total dissolved solids (TDS) and electrical conductivity (EC) of glacier meltwater was carried out according to the standard protocols of American Public Health Association (APHA, 2005) by using various calibrated standard instruments. The TDS of the meltwater was measured by a portable instrument (PCS tester 35) and the EC and pH were measured using New Professional Trimeter meters. Before taking measurements, the pH meter was calibrated using two standard buffer solution (pH 4.0 and 7.0) and EC meter was calibrated using a standard solution (1430 μ S/cm). The total discharge of the meltwater was calculated in the field by using area velocity method (Eq. 1). The flow velocity and cross sectional areas were calculated by the standard surveying technique as described by Hubbard and Glassar (2005) (Figure 2d). The meltwater discharge (Q) was calculated using the following formula (Hubbard & Glassar, 2005).

$$Q = k(A \times V)(1)$$

Where Q is meltwater discharge, k is correction factor (0.8) for calculating mean channel velocity, A is cross sectional area of the channel and V is the surface velocity of the flow.

Laboratory measurements

Hydrogeochemical analysis

The hydrogeochemical analysis of meltwater samples was carried out using a standard method (APHA, 2005). The sodium (Na⁺) and potassium (K⁺) concentration were determined in a single aspiration of sample through the help of Flame Photometer (Systronics flame photometer 128). The concentration of magnesium (Mg²⁺) and calcium (Ca²⁺) were determined by EDTA titration method and the chloride (Cl⁻) and Bicarbonate (HCO₃⁻) were measured by acid titration method. The concentration of sulfate (SO₄²⁻) and fluoride (F⁻) were analyzed using a photometer (Paqualb photometer 5000) and spectrophotometer (Eppendorf AG 22331) respectively. The Rock Ware, Inc. AqQA software version 1.5 was used for plotting piper diagram to identify the hydrochemical facies. The Statistical Package for Social Science (SPSS) version 10.5 was used to determine pearson correlation matrix between different physicochemical parameters.

Petrographic analysis

As mentioned in the text, the bedrock of the catchment area comprises of granites, gneisses, schist and metasediments. Thin sections of four different rock samples were prepared for petrographic analysis. The rock samples were cut into rectangular blocks and one side polished for adherence to glass specimen plates. After the samples were glued to the glass specimen plates, the sample blocks were then rubbed until an even surface (0.3 mm thickness) was obtained. The petrographic study of these thin sections was then undertaken

in petrographic microscope under transmitted light. Furthermore a detailed petrography was conducted and the approximate mineral assemblages were calculated through point counting technique by taking 500 points for each slide using Gazzi-Dickinson method (Gazzi, 1966; Dickinson, 1970).

Result and discussions

Hydrogeochemistry of glacier meltwater

The hydrogeochemical analysis of meltwater was carried out to assess the major ion chemistry and contribution of weathering process in dissolved ions. Various physical and chemical parameters of meltwater with maximum, minimum, average and standard deviation (STDEV) are shown in Table 1. The pH values of the meltwater ranges between 3.97 and 6.06 (average 5.5 ± 0.55) for 2015 and 4.61 to 6.32 (mean 5.81 ± 0.4) for 2016 (Table 1), showing that it is slightly acidic in nature. The electrical conductivity (EC) of meltwater ranges between 123.6 to 194.7 μ S/cm (average 173.6 \pm 21.74 μ S/cm) for the year 2015 and 118.52 to 191.9 μ S/cm (average $157.3\pm9.33 \ \mu\text{S/cm}$) for the year 2016 (Table 1). The EC mainly depends on the concentration of total dissolved solids (TDS) in the glacier meltwater (Bisht, Sah, Kumar, Arya, & Tewari, 2017; Singh, Ramanathan, Sharma, & Pottakkal, 2015) and is considered as a measure of TDS which generally depends on the ionic potential of the solution (Sharma, Ramanathan, & Pottakkal, 2013). The TDS of meltwater varied from 63.36 to 101.05 mg/L (average 89.82 ± 11.53 mg/L) in 2015 and 59.54 to 99.55 mg/L (average $81.12 \pm 4.97 \text{ mg/L}$ in 2016. High variability in EC also indicates that the catchment hydrogeochemistry is mainly controlled by rock water interaction and meteorological parameters (Kumar et al., 2018). Our results show higher average values of EC and TDS during the ablation season in 2015, compared to that in 2016. This is probably due to lower values of discharge in 2015 than in 2016 (Tables 2-3). This is because during less discharge, the meltwater has higher dissolved ion concentration due to longer contact and high residence time of meltwater with the basal lithology (Bisht et al., 2017; Singh et al., 2014a). Singh et al. (2014a) also suggested that lower discharge increases the concentration of TDS, while the higher discharge dilutes the TDS of the meltwater. Thomas, Joseph and Thrivikramji (2015) suggested that the lower values of EC in the glacier meltwater are due to increasing pattern of discharge through precipitation.

The cationic concentration of meltwater indicates that the average concentration of Ca^{2+} , Mg^{2+} , Na^+ and K^+ was 11±3.24, 10.8±4.07, 9.2±4.67 and 5.85±1.12 mg/L respectively in year 2015 and 9.6±4.12, 2.76±1.26, 5.6±3.4 and 3.12±1.15 respectively in year 2016. Similarly the average anionic concentration of meltwater indicate that the average concentration of HCO_3^- , SO_4^{2-} , CI^- and F^- was 188.49±12.6, 38.88±4.6, 2.8±1.29 and 0.38±0.16 mg/L respectively in year 2015 and 129.88±18.82, 26.88±1.95, 3.85±0.7 and 0.29±0.1 mg/L respectively in year 2016. This shows that Ca^{2+} is the most dominant cation in the meltwater followed by Mg^{2+} , Na^+ and K^+ which contribute 29.87%, 29.31%, 24.96%, and 15.86% of the total cations respectively in year 2015, while Ca^{2+} is the most dominant cation followed by Na^+ , K^+ and Mg^{2+} , contributing 45.54%, 26.55%, 14.82%, and 13.09% of the total cations, respectively in year 2016. Among the anions HCO₃⁻ is the most leading anion followed by SO_4^{2-} , CI^- and F^- which contribute 81.75%, 16.86%, 1.22%, and 0.17% of the total anions respectively in 2015 and 80.72%, 16.71%, 2.39%, and 0.18% of the total anions respectively in 2016.

Sources of solutes in the meltwater

Generally the concentration of dissolved ions in glacier meltwater depends on the mineralogy of bedrock, weathering reactions, composition and amount of atmospheric inputs and meltwater discharge (Singh & Hasnain, 1998). The mineralogy of surrounding rocks is necessary to understand better, the rock–water interaction processes, and their contribution in ionic concentration of meltwater (Bisht et al., 2018). The petrographic analysis shows that biotite $[K(Mg,Fe)_3AlSi_3O_{10}(OH)_2]$, alkali feldspar $[KAlSi_3O_8]$, plagioclase feldspar $[NaAlSi_3O_8 \text{ or } CaAl_2Si_2O_8]$ and quartz [SiO2] are the most abundant minerals in the deformed metasedimentary rocks. The Martoli formation metasediments and biotite granite near the snout are found with small amount of staurolite $[Fe_2Al_9O_6(SiO_4)_4(O,OH)_2]$ and garnet $[Mg_3Al_2Si_3O_{12}]$ (Figures 4 a-c) were found. The tourmaline $[Na(Mg,Fe)_3Al_6(BO_3)_3Si_6O_{18}(OH)_4]$, alkali feldspar $[KAlSi_3O_8]$, plagioclase feldspar $[NaAlSi_3O_8 \text{ or } CaAl_2Si_2O_8]$ and quartz [SiO2] are the most abundant mineral feldspar $[NaAlSi_3O_8]$, plagioclase feldspar $[NaAlSi_3O_8 \text{ or } CaAl_2Si_2O_8]$ and quartz [SiO2] are the most abundant mineral in tourmaline leucogranite $[NaAlSi_3O_8 \text{ or } CaAl_2Si_2O_8]$ and quartz [SiO2] are the most abundant mineral in tourmaline leucogranite $[NaAlSi_3O_8 \text{ or } CaAl_2Si_2O_8]$ and quartz [SiO2] are the most abundant mineral in tourmaline leucogranite $[NaAlSi_3O_8 \text{ or } CaAl_2Si_2O_8]$ and quartz [SiO2] are the most abundant mineral in tourmaline leucogranite $[NaAlSi_3O_8 \text{ or } CaAl_2Si_2O_8]$ and quartz [SiO2] are the most abundant mineral in tourmaline leucogranite $[NaAlSi_3O_8 \text{ or } CaAl_2Si_2O_8]$ and quartz [SiO2] are the most abundant mineral in tourmaline leucogranite $[NaAlSi_3O_8 \text{ or } CaAl_2Si_2O_8]$ and quartz [SiO2] are the most abundant mineral in tourmaline leucogranite $[NaAlSi_3O_8 \text{ or } CaAl_2Si_2O_8]$ and quartz [SiO2] are the most abundant mineral in tourmaline leucogranit

lithotype (Figure 4d). The results suggest that K⁺ has definitely entered into the meltwater due to weathering of alkali feldspar and biotite. The Ca^{2+} has contributed in the meltwater due to plagioclase feldspar while Na^+ is due to alkali feldspar, plagioclase feldspar and tournaline. The Mg^{2+} is added in the meltwater is due to weathering of biotite, garnet and tourmaline. Based on the petrographic analysis, we suggest that the cations such as Ca²⁺, Mg²⁺, Na⁺ and K⁺show a good relationship with the mineral abundance of the rocks. The main sources of dissolved ions and mechanism controlling hydrogeochemistry of glacier meltwater can also be assessed on the basis of relationship among the ions and their ratios (Bisht et al., 2018; Kumar et al., 2019; Sharma et al., 2013). The scatter plot between (Ca + Mg) and TZ^+ (Figure 5) shows that all plotted points fall above the 1:1 equiline with an average ratio of (0.59 ± 0.02) in 2015 and (0.58 ± 0.04) in 2016 (Table 1). Similarly, the (Ca+Mg)/(Na+K) ratios were found as 1.47 \pm 0.14 in 2015 and 1.44 \pm 0.28 in 2016. On the other hand, the scatter plot between Na+K and TZ (Figure 6) shows that all points lie below 1:1 equiline with low elemental ratios were 0.41 ± 0.02 in 2015 and 0.22 ± 0.05 in 2016 (Table 1). The high Ca+Mg/TZ and (Ca+Mg)/(Na+K) ratios and low Na+K/TZ ratios for both the years indicate that carbonate weathering is the dominant mechanism controlling the hydrogeochemistry of the Chaturangi glacier meltwater with diminutive contribution by silicate weathering. The scatter plot between (Ca + Mg)and SO_4^{2-} (Figure 7) shows most of the points fall above the 1:1 equiline which indicates that MgSO₄ and $CaSO_4$ rich rocks are main sources for supply of sulphate in the meltwater. Singh et al. (2014b) suggested that the oxidation of sulphides could be a second possible source of sulphate in the meltwater. The occurrence of sulphide minerals like pyripte and chalcopyrite at the contact quartz veinlets in country rocks near the glacier snout (Bhatt, 1963) indicates that oxidation of sulphides is one of the major source of sulphate in the meltwater of Chaturangi glacier. The water draining from carbonate lithology shows high concentration of Ca²⁺ and Mg²⁺ as well as high ratios of HCO₃/Na (120), Ca/Na (50) and Mg/Na (10) (Negrel, Allegre, Dupre, & Lewin, 1993), whereas, the water draining from silicate lithology shows less ratios of HCO_3/Na (2), Ca/Na (0.35) and Mg/Na (0.24) (Gaillardet, Dupre, Louvat, & Allegre, 1999). In the present study, we observed ratios of HCO_3/Na as 24.69±9.05 in 2015 and 28.31±9.84 in 2016. We also found the Ca/Na as 1.31 ± 0.27 in 2015 and 1.83 ± 0.87 in 2016 as well as Mg/Na as 1.25 ± 0.21 in 2015 and 0.54 ± 0.19 in 2016. The result shows that HCO3/Na, Ca/Na and Mg/Na ratios of the meltwater are in accordance that the lithologies are influencing the hydrogeochemisty of Chaturangi glacier meltwater.

Although chemical weathering of rocks are the main sources of dissolved ions in the meltwater but atmospheric precipitation may also have a contribution to the total dissolved ions (Singh et al., 2014b). A few studies are available on the contribution of atmospheric input to the meltwater chemistry of Central Himalayan glaciers (Kumar et al., 2009; Singh et al., 2014a; Tiwari et al., 2018). It is known that the atmospheric contribution to the meltwater chemistry is best studied by the assessment of element-to-chloride ratio in the meltwater (Kumar et al., 2009). Therefore, in order to determine the contribution of atmospheric input into the meltwater chemistry of Chaturangi glacier, the element-to-chloride ratio was studied during the ablation seasons of 2015 and 2016. The scatter plot between Na+K and Cl⁻(Figure 8) shows that Na+K concentration is higher than chloride in year 2015, while it is lowered in 2016. The average K/Cl ratios in the Chaturangi meltwater were found as 2.29 ± 0.62 in 2015 and 0.8 ± 0.2 in 2016, whereas, the average Na/Cl ratios were 3.36 ± 1.29 in 2015 and 1.39 ± 0.6 in 2016. The K/Cl and Na/Cl ratios are significantly much higher than those for marine aerosols (i.e. K/Cl = 0.0176 and Na/Cl = 0.85) in 2015 and slightly higher in 2016 (Table 1). Hence, it clearly shows relatively small contribution of these ions in the meltwater from atmospheric input in both the years. Furthermore, the results also show relatively high contribution of ions in the meltwater from the atmosphere in 2016, compared to that in 2015. Similar results of low contribution of ions in the meltwater of Himalayan glaciers from atmospheric precipitation are reported by other workers (Bisht et al., 2018; Kumar et al., 2009; Sharma et al., 2013; Singh et al., 2015; Singh, Keshari, & Ramanathan, 2019; Singh & Ramanathan, 2017). It clearly indicates that major portion of dissolved ions in meltwater of the Chaturangi glacier is mainly controlled by weathering of rock forming minerals. The proton source must be required for the chemical weathering of carbonate rocks (Khadka & Ramanathan, 2012). In the stream water, the concentration of HCO_3^- and SO_4^{2-} reflects the dominance of the two main sources of aqueous protons driving the sub-glacial weathering reactions (Brown, Tranter, & Sharp, 1996; Hasnain & Thayyen, 1999; Raiswell, 1984).

 $\begin{aligned} &CO_2 + H_2O \ H_2CO_3 \ (2) \\ &H_2CO_3 \ H^+ + HCO_3^- \ (3) \\ &CaCO_3 \ (s) + H_2CO_3 \ (aq) \ Ca^{2+} \ (aq) + 2HCO_3^- (aq) \ (4) \\ &4FeS_2(s) + 16CaCO_3(s) + 15O_2(aq) + 14H_2O \ (l) \ 16Ca^{2+} (aq) + 16HCO_3^- (aq) + 8SO_4^{2-} (aq) + 4Fe(OH)_3(s) \ (5) \end{aligned}$

Importance of two proton producing reactions, i.e., carbonation and sulfide oxidation are crucial components for weathering of carbonate rocks and this is best explained by C-ratio $[(\text{HCO}_3/(\text{HCO}_3+\text{SO}_4)]$ (Brown et al., 1996; Huang, Sillanpää, & Gjessing, 2008). If C ratio is close to 1, it represents chemical weathering by carbonation reaction (Equations 2-4). If this ratio is close to 0.5, it signifies the coupled reaction involving carbonate dissolution and sulphide oxidation with protons derived from the oxidation reaction of pyrite (Equation 5) (Brown et al., 1996). Similarly, the S ratio $[\text{SO}_4/(\text{SO}_4+\text{HCO}_3)]$ close to 0.5 shows weathering by coupled reaction involving carbonate dissolution and sulphide oxidation, whereas, the ratio near 0 indicates chemical weathering by carbonation reaction (Tranter et al., 1997). The average C-ratio for Chaturangi glacier meltwater was 0.83 ± 0.009 in 2015 and 0.83 ± 0.01 in 2016 and this shows that the chemical weathering in the area is mainly controlled by the carbonate rocks and disassociation of atmospheric CO₂. Further, the average S-ratio for Chaturangi glacier meltwater was 0.17 ± 0.009 in 2015 and 0.10 ± 0.02 in 2016 and this also confirms that the chemical weathering in the area is mainly controlled by carbonate rocks and disassociation of atmospheric CO₂. Further, the

The ratio of TDS (mg/l) to EC (μ s/cm) is commonly accepted as 0.7 for fresh water (Meybeck, 1984). In the Chaturangi, average TDS/ EC ratio was 0.515 in 2015 and 0.517 in 2016 which is in agreement that the water is slightly fresh in nature. In addition, the concentration F⁻ in the meltwater has also been observed to determine the drinking water quality of meltwater. The average value of F⁻ was 0.38±0.16 mg/L in 2015 and 0.29±0.1 mg/L in 2016 (Table 1). In both the years the average concentration of F⁻ in Chaturangi glacier meltwater is relatively low as compared to the maximum permissible limit (1.5 mg/L) given by Bureau of Indian Standards (BIS, 1991), which shows that the meltwater is acceptable for drinking in respect to fluoride contamination. The replacement of ions of crystal lattice of micas and other mineral might be the possible sources of F⁻ in the water (Sadat, 2012).

Ionic flux and denudation rate of ions

In this study, we have calculated the ionic flux to the meltwater stream from the streambed and denudation rate of the ions through meltwater from the Chaturangi glacier catchment during the whole ablation seasons in 2015 and 2016. The cationic flux (Fx^+) and cation denudation rate (R^+) was calculated by using the following formula (Fang, Zhongqin, Shuang, Jhiwen, & Feiteng, 2012):

$$Fx^{+} = \sum_{i=1}^{n} C_{i}^{+}(t) \times Q(t) \quad (6)$$
$$R^{+} = \frac{Fx^{+}}{m} \quad (7)$$

Where C_i^+ is concentration of cations (Ca²⁺, Mg²⁺, Na⁺ and K⁺) in the meltwater, Q is meltwater discharge, t refers to a particular time period and m represents catchment area. Similarly, the anionic flux (Fx^-) and anion denudation rate (R^-) were also calculated.

The ionic flux, ion denudation rate, meltwater discharge of Chaturangi glacier and catchment area during 2015 and 2016 are given in Tables 2-3. The glacier catchment covers an area of about 214.8 km² (Orr et al., 2019) with an average discharge 1.91×10^{11} litre and 2.27×10^{11} litre during the ablation season of 2015 and 2016 respectively. The total cationic flux as 59.76 ton per day and 7053.06 ton per ablation season was observed in 2015, whereas, it was measured as 39.26 ton per day and 4790.70 ton per ablation season in 2016. On the other hand, the total anionic flux as 373.94 ton per day and 44127.12 ton per ablation season were observed in 2015, whereas 299.72 ton per day and 36566.63 ton per ablation period were measured in 2016. The results show that calcium contributes the highest cationic flux as 29.85 % and 45.54 % of total cations in 2015 and 2016 respectively, as well as the bicarbonate contribute highest anionic flux as 81.76 % and 80.72 % of total anions in 2015 and 2016 respectively. In addition, the cation denudation rate as

 $0.28 \text{ ton/km}^2/\text{day}$ and $32.84 \text{ ton/km}^2/\text{ablation}$ were observed in 2015, while $0.18 \text{ ton/km}^2/\text{day}$ and $22.30 \text{ ton/km}^2/\text{ablation}$ were observed in 2016. Furthermore, the anion denudation rate as $1.74 \text{ ton/km}^2/\text{day}$ and $205.43 \text{ ton/km}^2/\text{ablation}$ were measured in 2015, whereas, it was found as $1.40 \text{ ton/km}^2/\text{day}$ and $170.24 \text{ ton/km}^2/\text{ablation}$ in 2016. The ionic flux as well as the denudation rate of the ions is higher in 2015 as compared to 2016, probably due to variation in discharge. Thus, our results suggest that the ionic flux and denudation rate of the ions are largely dependent on the glacier meltwater discharge and as soon as the meltwater discharge increases, the ionic weathering rate tends to increase as well.

Hydrogeochemical facies of meltwater and effective CO₂ pressure

The Piper plot is important to establish a relationship between rock type and composition of water by plotting the value of major ions (Ca²⁺, Mg²⁺, K⁺, Na⁺, HCO₃⁻, SO₄²⁻ and Cl⁻) (Singh et al., 2014a). We have plotted a trilinear diagram to identify the hydrogeochmical facies of meltwater draining from the Chaturangi in 2015 and 2016. The plot contains one quadrilateral (rhombus) shaped diagram at the top and two triangular shaped diagrams on its left and right at the bottom (Figure 9). The results obtained from the Piper plot shows that the Mg-HCO₃ and Ca-HCO₃dominated hydrogeochemical facies were present in the study area in 2015 and 2016 respectively. Variability in the hydrogeochemical facies in 2015 and 2016 may be attributed to interaction time between minerals and flowing water, because of gradual changes in meltwater discharge during the study period. The piper plot (Figure 9) also shows that alkaline earth metals (Ca+Mg) exceed over alkalis (Na+K) and weak acid (HCO₃) exceeds over strong acid (SO₄+Cl) for most of the samples for both the years. Such a combination confirms that major source of dissolved ions in Chaturangi glacier meltwater is carbonate weathering followed by silicate weathering. The gibbs diagram is plotted to assess the dominated hydro-geochemical facies and water quality controlling mechanism of the catchment area (Kumar, Logeshkumaran, Magesh, Godson, & Chandrasekar, 2015). It is also used to establish a relationship between water composition and lithological characteristics. The Gibbs plots [TDS vs Na/(Na+Ca) and TDS vs $Cl/(Cl+HCO_3)$] show that the most samples fall in the rock water interaction dominance zone and also tend towards the precipitation dominance zone (Figure 10). This clearly indicates that weathering of rocks mainly control the solute concentration of Chaturangi glacier meltwater with little contribution from the precipitation.

The partial pressure of carbon dioxide or effective CO_2 pressure (pCO₂) of glacier meltwater can be used to describe different hydrological weathering environments (Sharp, Tranter, Brown, & Skidmore, 1995; Wadham, Hodson, Tranter, & Dowdeswell, 1998). The open and closed system weathering environments are kinetic phenomena, and depend on the factors which influence the weathering rates (i.e. rock minerals availability and reactivity) and the rate of extent of CO_2 transfer to the meltwater draining from the glaciers (Raiswell, 1984; Thomas & Raiswell, 1984). The pCO₂ of water reflects the rate of CO₂diffusion relative to the rate of other weathering reactions (Thomas & Raiswell, 1984). The low pCO_2 values in the solution seem appeared when the requirement of protons (H^+) for chemical weathering is higher than the rate of CO_2 diffusion, whereas the high pCO_2 values were appeared when the supply of proton is higher into the solution than they consumed (Tranter, Brown, Raiswell, Sharp, & Gurnell, 1993; Wadham et al., 1998). The pCO₂ has been calculated through the help of HCO₃ and pH values of the water (Stumm & Morgan, 1981). The average values of pCO_2 for Chaturangi glacier meltwater were $10^{-1.2}$ in 2015 and $10^{-1.39}$ in 2016 which is higher than the pCO_2 values of atmosphere (10^{-3.5}). The higher pCO_2 values of meltwater than atmosphere in both the years is probably due to low temperature, high turbulence, open system weathering and carbonate weathering processes (Ahmad & Hasnain, 2001; Singh et al., 2012). However, our results indicate that the open system of weathering and higher solubility of CO_2 in the meltwater as well as it also suggested that the meltwater is in disequilibrium state with respect to the surrounding atmosphere.

Statistical analysis

Statistical analysis such as correlation matrix is a bivariate method mainly used to determine the relationship between two hydrogeochemical parameters for investigating the dependability of different variables among each other (Thilagavathi, Chidambaram, Prasanna, Thivya, & Singaraja, 2012; Bisht et al., 2018). Therefore, the correlation matrix could be helpful in evaluating the water quality of various environments. A

multi-parametric correlation matrix between measured hydrogeochemical parameters of Chaturangi glacier meltwater samples for year 2015 (a) and 2016 (b) is presented in Table 4. The correlation matrix shows that the EC has a strong positive correlation with TDS and pH during both the years (Table 4). It indicates that EC is directly related to ions dissolved in the meltwater through surrounding rocks, soil and atmosphere. The strong correlation was observed between Ca^{2+} and Mg^{2+} ($r^2=0.93$ in 2015 and $r^2=0.85$ in 2016), Ca^{2+} and $HCO_3^-(r^2=0.85$ in 2015 and $r^2=0.94$ in 2016) and Mg^{2+} and HCO_3^- ($r^2=0.89$ in 2015 and r^2 = 0.84 in 2016), indicating similar source, i.e. carbonate weathering. The Na⁺ showed moderate correlation ($r^2 = 0.63$) with K⁺ in 2015 as well as little bit higher correlation ($r^2 = 0.71$) in 2016, indicating similar source of both the chemical species, i.e. partial silicate weathering in Chaturangi glacier catchment.

Further, the factor analyses for different variables which were measured from the Chaturangi glacier meltwater for both the years are presented in Table 5. Factor analysis is a useful statistical method that used to explain the relationship between the different analyzed variables by the computation of various multivariate factors and by reducing the complex data to an easily interpretable data (Davis, 2002; Patel et al., 2017). Factor analysis is also called the principal component analysis which is also helpful for the visualization and management of complex system of data, when similarities of data and patterns are not well understood (Valder, Long, Davis, & Kenner, 2012). In present study the varimax rotation has been used for factor analysis which is commonly useful in most of the hydrogeochemical studies. To extract the significant contributing factors, we have used only those factors that have the eigen value greater than one. The two major contributing factors were obtained from the factor analysis in both the years which explained 85.08%and 84.16% of the total cumulative variance in year 2015 and 2016 respectively. During the ablation season in 2015 the factor 1 shows strong positive loading of HCO₃⁻, F⁻, SO₄²⁻, Na⁺, Ca²⁺ and Mg²⁺with 49.30% of the variance in the dataset (Table 5). This factor indicates contribution of dissolved ions from weathering of carbonate minerals and dissolution of sulphate minerals. The factor 2 shows high loading of EC, pH, Cl⁻ and K^+ with 35.79% of the variance (Table 5). This factor reflects contribution of these parameters mainly from the weathering of silicate minerals and atmospheric input. Further for the ablation period of 2016 the factor 1 shows strong positive loading of EC, pH, HCO₃⁻, SO₄²⁻, Ca²⁺ and Mg²⁺ with 45.58% of the variance (Table 5). This factor indicates the contribution of these parameters mainly from the weathering of carbonate minerals and sulphate dissolution. The factor 2 shows high positive loading of F⁻, Cl⁻, Na²⁺, Ca^{2+} and K^{+} with 38.57% of the variance in the data (Table 5). This indicates the contribution of these ions mainly from the silicate weathering and atmospheric deposition.

Conclusion

The analysis of Chaturangi glacier meltwater samples collected during the ablation seasons of 2015 and 2016 were carried out to understand the hydrogeochemical processes regulating the major ion chemistry of meltwater. Furthermore the study also gives insight on the chemical weathering process and mineralogy of surrounding rocks to identify the ionic sources and factors controlling the ionic composition of meltwater. The hydrogeochemical study of meltwater samples indicates that the meltwater is slightly acidic in nature with Mg-HCO₃ and Ca-HCO₃ dominated hydrochemical facies in year 2015 and 2016 respectively. The concentration of cations in the meltwater sample shows that Ca^{2+} is the most dominant cation followed by Mg^{2+} , Na^+ and K^+ in 2015, while Ca^{2+} is the most dominant cation followed by Na^+ , K^+ and Mg^{2+} in 2016. Among the anions HCO_3^- is the most dominant anion followed by SO_4^{2-} , Cl^- and F^- in both the years. The variations in dissolve ion concentration during the ablation season of two different years were observed which is probably being due to variability of meltwater discharge. The comparatively higher contribution of (Ca+Mg) in total cations and higher elemental ratio of (Ca+Mg)/(Na+K) clearly indicate that chemical composition is mainly controlled by carbonate weathering and partly by silicate weathering. Furthermore the low elemental ratio of $(Na+K)/TZ^{-}$ also suggest that carbonate weathering is a dominant geochemical process to controlling meltwater chemistry. The correlation matrix and factor analysis also indicate that hydrogeochemical characteristics of the meltwater are mainly controlled by the weathering processes with a minor contribution of atmospheric precipitation. The C ratio and S ratio of the glacier meltwater shows that the weathering is mainly controlled by carbonation reactions. In addition the average equivalent ratio of Na/Cl and K/Cl of meltwater is significantly higher than those of marine aerosols indicate that the low

contribution of atmospheric input in glacier meltwater. The gibbs plot also suggested that ionic concentration of meltwater is mainly controlled by rock weathering and little contribution from the atmosphere. The results derived from the petrographic analysis suggest that the rocks near the snout of the glacier are rich in alkali feldspar, plagioclase feldspar, biotite, quartz with some amount of tourmaline, garnet, staurolite, pyrite and chalcopyrite, which contribute the major cations and anions reflected in the hydrochemistry of meltwater. The higher pCO₂ values of Chaturangi glacier meltwater than atmosphere indicate that the open system of weathering and higher solubility of CO₂ in the meltwater. Further it also suggested that the meltwater is in disequilibrium with respect to the surrounding atmosphere. To assess the effectiveness of chemical denudation, an estimation of solute fluxes suggested that cation denudation rate of meltwater runoff of Chaturangi glacier were 32.84 and 22.30 ton/km²/ablation during 2015 and 2016 respectively, whereas the anion denudation rate were 205.43 and 170.24 ton/km²/ablation in 2015 and 2016 respectively.

References

Ahmad, S., & Hasnain, S. I. (2001). Chemical characteristics of stream draining from Dudu glacier: an Alpine meltwater stream in Ganga Headwater, Garhwal Himalaya. *Journal of China University of Geoscience*, 12 (1), 75-83.

APHA (American Public Health Association) (2005). Standard methods for examination of water and waste water, 21st edn. American Public Health Association, Washington, DC.

Bali, R., Awasthi, D. D., & Tiwari, N. K. (2003). Neotectonic control on the geomorphic evolution of the Gangotri Glacier Valley, Garhwal Himalaya. *Gondwana Research*, 6(4), 829-838. https://doi.org/10.1016/S1342-937X(05)710285

Bhatt, B. K. (1963). Preliminary study of the Bhagirathi basin between Uttarkashi and Gomukh. In Proceeding National Symposium. On Himalayan Geology, Calcutta. *Geological Society of India Miscelaneous Publicaion*, 15, 1-8.

Bisht, H., Arya, P. C., & Kumar, K. (2018). Hydro-chemical analysis and ionic flux of meltwater runoff from Khangri Glacier, West Kameng, Arunachal Himalaya, India. *Environmental Earth Sciences*, 77,1-16. https://doi.org/10.1007/s1266 5-018-7779-6

Bisht, H., Kotlia, B. S., Kumar, K., Arya, P. C., Sah, S. K., Kukreti, M., & Chand, P. (2020a). Estimation of suspended sediment concentration and meltwater discharge draining from the Chaturangi glacier, Garhwal Himalaya. *Arabian Journal of Geosciences*, 13(6), 1-12. https://doi.org/10.1007/s12517-020-5204-w4

Bisht, H., Kotlia, B.S., Kumar, K., Joshi, L. M., Sah, S. K., & Kukreti, M. (2020b). Estimation of the recession rate of Gangotri glacier, Garhwal Himlaya (India) through kinematic GPS survey and satellite data. *Environmental Earth Sciences*, 13(6), 1-12. https://doi.org/10.1007/s12665-020-09078-0

Bisht, H., Rani, M., Kumar, K., Sah, S., & Arya, P. C. (2019). Retreating rate of Chaturangi glacier, Garhwal Himalaya, India derived from kinematic GPS survey and satellite data. *Current Science*, 116, 304-311. https://doi.org/10.18520/ cs/v116/i2/304-311

Bisht, H., Sah, S., Kumar, K., Arya, P. C., & Tewari, M. (2017). Quantification of variability in discharge and suspended sediment concentration of meltwater of Gangotri glacier, Garhwal Himalaya. *ENVIS Bulletin Himalayan Ecology*, 25, 10-16.

Bolch, T., Kulkarni, A., Kääb, A., Huggel, C., Paul F, Cogley, J. G., ... Stoffel, M. (2012). The state and fate of Himalayan glaciers. *Science*, 336(6079), 310-314. https://doi.org/10.1126/science.1215828

Brown, G. H., Tranter, M., & Sharp, M. (1996). Subglacial chemical erosion- seasonal variations in solute provenance, Haut glacier d'Arolla, Switzerland. Annals of Glaciology, 22, 25-31. https://doi.org/10.3189/1996AoG22-1-25-31

BIS (Bureau of Indian Standards) (1991). Indian standards drinking water specification IS 10500.

Carling, G. T., Rupper, S. B., Fernandez, D. P., Tingey, D. G., & Harrison, C. B. (2017). Effect of atmospheric deposition and weathering on trace element concentrations in glacial meltwater at Grand Teton National Park, Wyoming, USA. Arctic, Antarctic, and Alpine Research, 49(3), 427-440.

Clow, D. W., Mast, M. A. (2010). Mechanisms for chemostatic behavior in catchments: implications for CO2 consumption by mineral weathering. *Chemical Geology*, 269, 40-51. https://doi.org/10.1016/j.chemgeo.2009.09.014

Collins, D. N. (1979). Hydrochemistry of meltwater draining from an Alpine glacier. Arctic, Antarctic and Alpine Research, 11,307-324. https://doi.org/10.3189/S0022143000029877

Davis, J. C. (2002). *Statistics and Data Analysis in Geology*. John Wiley and Sons, New York. https://doi.org/ 10.1180/minmag.1976.040.315.20

Dickinson, W. R. (1970). Interpreting detrital modes of greywake and arkose. *Journal of Sedimentary Petrology*, 40, 695-707.

Dimri, A. P., Yasunari, T., Kotlia, B. S., Mohanty, U. C., & Sikka, D. R. (2016). Indian Winter Monsoon; Present and Past. *Earth Science Review*, 163, 297-322. https://doi.org/10.1016/ j.earscirev.2016.10.008

Dyurgerov, M. B., & Meier, M. F. (1997). Twentieth century climate change: Evidence from small glaciers. Proceedings of National Academy of Sciences of the United States of America, 97, 1406-1411.

Fang, F., Zhongqin, L., Shuang, J., Jhiwen, D., & Feiteng, W. (2012). Hydrochemical characteristics and solute dynamics of meltwater runoff of Urumqi Glacier No.1, Eastern Tianshan, Northwest China. *Journal of Mountain Science*, 9, 472-482. https://doi.org/10.1007/s11629-012-2316-7

Gaillardet, J., Dupre, B., Louvat, P., & Allegre, C. J. (1999). Global silicate weathering and silicate weathering and CO2 consumption rates deduced from the chemistry of large rivers. *Chemical Geology*, 159, 3-30.

Gazzi, P. (1966). Le Arenarie del Flysch Sopracretaceodell'Appennino Modenese: correlazioni conil Flysch di Monghidoro. *Mineralogica e Petrographica Acta, 12,* 69-97.

Godsey, S. E., Kirchner, J. W., & Clow, D. W. (2009). Concentration-discharge relationships reflect chemostatic characteristics of US catchments. *Hydrological Processess*, 23,1844-1864. https://doi.org/10.1002/hyp.7315

Hallet, B. (1976). Deposits formed by subglacial precipitation of CaCO₃. *Geological Society of American Bulletin*, 87, 1003-1015.

Hasnain, S. I., & Thayyen, R. J. (1999). Discharge and suspended-sediment concentration of meltwaters, draining from the Dokriani glacier, Garhwal Himalaya, India. *Journal of Hydrology*, 218, 191-198. htt-ps://doi.org/ 10.1016/ s00221694(99)00033-5

Huang, X., Sillanpää, M., Duo, B., & Gjessing, E. T. (2008). Water quality in the Tibetan Plateau: metal contents of four selected rivers. *Environmental Pollution*, 156(2), 270-277.

Hubbard, B., & Glassar, N. (2005). Field techniques in glaciology and glacial geomorphology. John Wiley and Sons, England.

Khadka, U. R., & Ramanathan, A. L. (2012). Major ion composition and seasonal variation in the Lesser Himalayan lake: case of Begnas Lake of Pokhara Valley, Nepal. Arabian Journal of Geosciences, 7(4),1-10.

Krishnaswami, S., & Singh, S. K. (2005). Chemical weathering in the river basins of the Himalaya, India. *Current Science* 89(5),841-849.

Kulkarni, A.V., & Karyakarte, Y. (2014). Observed changes in Himalayan glaciers. *Current Science*, 106(2), 237-244.

Kumar, K., Miral, M. S., Joshi, S., Pant, N., Joshi, V., & Joshi, L. M. (2009). Solute dynamics of meltwater of Gangotri glacier, Garhwal Himalaya, India. *Environmental Geology*, 58(6), 1151-1159. htt-ps://doi.org/10.1007/ s00254-008-1592-6

Kumar, R., Kumar, R., Singh, A., Singh, S., Bhardwaj, A., Kumari, A., ... Gupta, A. (2019). Hydrogeochemical analysis of meltwater draining from Bilare Banga glacier, Western Himalaya. *Acta Geophysica*, 67(2), 651-660. https://doi.org/10.1007/s11600-019-00262-w

Kumar, R., Singh, S., Singh, A., Bhardwaj, A., Kumari, A., Randhawa, S. S., & Saha, A. (2018). Dynamics of suspended sediment load with respect to summer discharge and temperatures in Shaune Garang glacierized catchment, Western Himalaya. *Acta Geophysica*, 66, 1109-1120.

Kumar, S. K., Logeshkumaran, A., Magesh, N. S., Godson, P. S., & Chandrasekar, N. (2015). Hydrogeochemistry and application of water quality index (WQI) for groundwater quality assessment, Anna Nagar, part of Chennai city, Tamil Nadu, India. *Applied Water Science*, 5,335-343. https://doi.org/10.1007/s13201-014-0196-4

Meybeck, M. (1984). Atmospheric inputs and river transport of dissolve substances. In B. W. Webb (Ed.), *Dissolved loads of rivers and surface water quantity/quality relationships* (pp. 173-192). IAHS Publication, Wallingford.

Negrel, P., Allegre, C. J., Dupre, B., & Lewin, E. (1993). Erosion sources determined by inversion of major and trace element ratios in river water: The Congo basin case. *Earth Planetary Science Letter*, 120, 59-76. https://doi.org/10.1016/0012-821X(93)90023-3

Noh, H., Huh, Y., Qin, J., & Ellis, A. (2009). Chemical weathering in the three rivers region of Eastern Tibet. *Geochimicaet Cosmochimica Acta*, 73, 1857-1877. https://doi.org/10.1016/j.gca.2009.01.005

Orr, E. N., Owen, L. A., Saha, S., & Caffee, M. W. (2019). Rates of rockwall slope erosion in the upper Bhagirathi catchment, Garhwal Himalaya. *Earth Surface Processess and Landforms*, 44, 3108-3127. https://doi.org/ 10.1002/eps.4720

Ostrem, G. (1975). Sediment transport in glacial meltwater stream. In A. V. Jopling, & B. C. McDonald (Eds.), *Glacio-fluvial and Glacio-lacustrine Sedimentation* (pp. 101-122). Society of Economic palaeontologists and Mineralogists.

Patel, K. S., Sahu, B. L., Dahariya, N. S., Bhatia, A., Patel, R. K., Matini, L., ... Bhattacharya, P. (2017). Groundwater arsenic and fluoride in Rajnandgaon District, Chhattisgarh, northeastern India. Applied Water Science, 7, 1817-1826. https://doi.org/ 10.1007/s13201-015-0355-2

Raina, V. K., & Srivastava, D. (2008). Glacier atlas of India. *Geological Society of India, Bangalore, Miscel*laneous publication, p 315.

Raiswell, R. (1984). Chemical models of solute acquisition in glacial meltwater. *Journal of Glaciology*, 30(104), 49-57. https://doi.org/10.1017/s0022143000008480

Ramanathan, A. L. (2011). Status report on Chhota Shigri Glacier (Himachal Pradesh). New Delhi: Department of Science and Technology, Ministry of Science and Technology, Himalayan Glaciology Technical Report Number 1

Raymo, M. E., Ruddiman, W. F. (1992). Tectonic forcing of late Cenozoic climate. *Nature, 359*, 117-122. https://doi.org/10.1038/359117a0

Sadat, N. (2012). Study of fluoride concentration in the river (Godavari) and groundwater of Nanded city. International Journal of Engineering Inventions, 1(1), 11-15.

Sah, S., Bisht, H., Kumar, K., Tiwari, A., Tewari, M., & Joshi, H. (2017). Assessment of hydrochemical properties and annual variation in meltwater of Gangotri glacier system. *ENVIS Bulletin Himalayan Ecology*, 25, 17-23.

Searle, M. P., Noble, S. R., Hurford, A. J., Rex, D. C. (1999). Age of crustal melting, emplacement and exhumation history of the Shivling leucogranite, Garhwal Himalaya. *Geological Magazine*, 136(5),513-525. https://doi.org/10.1017/s0016756899002885

Sharma, S., Chand, P., Bisht, P., Shukla, A. D., Bartarya, S. K., Sundriyal, Y. P., Juyal, N. (2016). Factors responsible for driving the glaciation in the Sarchu Plain, eastern Zanskar Himalaya, during the late Quaternary. *Journal of Quaternary Science*, 31(5), 495-511. https://doi.org/10.1002/jqs.2874

Sharma, P., Ramanathan, A. L., & Pottakkal, J. (2013). Study of solute sources and evolution of hydrogeochemical processes of the ChotaShigri Glacier meltwaters, Himanchal Himalaya, India. *Hydrological Sciences Journal*, 58(5), 1128-1143. https://doi.org/10.1080/02626667.2013.802092

Sharp, M., Tranter, M., Brown, G. H., & Skidmore, M. (1995). Rates of chemical denudation and CO₂ drawdown in a glacier-covered alpine catchment. *Geology*, 23(1), 61-64. https://doi.org/10.1130/00917613(1995) 023<0061:ROCDAC>2.3.CO;2

Shin, W., Ryu, J., Park, Y., & Lee, K. (2011). Chemical weathering and associated CO₂ consumption in six major river basins, South Korea. *Geomorphology*, 129, 334-341. https://doi.org/10.1016/j.geomorph.2011.02.028

Singh, A. K., & Hasnain, S. I. (1998). Major ion chemistry and weathering control in a high altitude basin: Alaknanda River, Garhwal Himalaya, India. *Hydrological Sciences Journal*, 436, 825-884. https://doi.org/ 10.1080/02626669809492181

Singh, V. B., Keshari, A. K., & Ramanathan, A. L. (2019). Major ion chemistry and atmospheric CO₂ consumption deduced from the Batal glacier, Lahaul–Spiti valley, Western Himalaya, India. *Environment Development and Sustainability*, 19, 1-19. https://doi.org/10.1007/s10668-019-00501-6

Singh, V. B., & Ramanathan, A. L. (2017). Hydrogeochemistry of the Chhota Shigri glacier meltwater, Chandra basin, Himachal Pradesh, India: Solute acquisition processes, dissolved load and chemical weathering rates. *Environmental Earth Sciences*, 76(5), 223-232. https://doi.org/ 10.1007/s1266 5-017-6465-4

Singh, V. B., Ramanathan, A. L., Pottakkal, J. G., & Kumar, M. (2014a). Seasonal variation of the solute and suspended sediment load in Gangotri Glacier meltwater, central Himalaya, India. *Journal of Asian Earth Sciences*, 79, 224-234. https://doi.org/10.1016/j.jseaes.2013.09.010

Singh, V. B., Ramanathan, A. L., Pottakkal, J. G., & Kumar, M. (2014b). Hydrogeochemisty of meltwater of the Chaturangi glacier, Garhwal Himalaya, India. *Proceedings National Academy of Science, India*, 85(1), 187-195. https://doi.org/ 10.1007/s40010-014-0181-1

Singh, V. B., Ramanathan, A. L., Pottakkal, J. G., Sharma, P., Linda, A., Azam, M. F., & Chatterjee, C. (2012). Chemical characterisation of meltwater draining from Gangotri Glacier, Garhwal Himalaya, India. *Journal of Earth System Science*, 121(3), 625-636.

Singh, V. B., Ramanathan, A. L., Pottakkal, J. G., Sharma, P., Linda, A., Chatterjee, C., ... Mandal, A. (2013). *Hydrochemistry of meltwater emerging from Raktvarn glacier, Central Himalaya, India*. Climate change and Himalayan ecosystem-indicator, bio and water resources, pp 109-118.

Singh, V. B., Ramanathan, A. L., Sharma, P., & Pottakkal, J. G. (2015). Dissolved ion chemistry and suspended sediment characteristics of meltwater draining from Chhota Shigri Glacier, western Himalaya, India. *Arabian Journal of Geosciences*, 8, 281-293. https://doi.org/10.1007/s12517-013-1176-y

Souchez, R. A., & Lemmens, M. M. (1987). Solutes. In A. M. Gurnell, & M. J. Clark (Eds.), *Glacio-fluvial* sediment transfer (pp. 285-303). Wiley, UK.

Stumm, W., & Morgan, J. J. (1981). An introduction emphasizing chemical equilibria in natural waters. In W. Stumm, & J. J. Morgan (Eds.), *Aquatic chemistry*, 2nd Edition (pp. 230-258). Wiley, New York.

Thayyen, R. J., Gergan, J. T., & Dobhal, D. P. (2007). Role of glaciers and snow cover on headwater river hydrology in monsoon regime-microscale study of Din Gad catchment, Garhwal Himalaya, India. *Current Science*, 92(3), 376-382.

Thilagavathi, R., Chidambaram, S., Prasanna, M. V., Thivya, C., & Singaraja, C. (2012). A study on groundwater geochemistry and water quality in layered aquifers system of Pondicherry region, southeast India. *Applied Water Science*, 2, 253-269. https://doi.org/10.1007/s13201-012-0045-2

Thomas, A. G., & Raiswell, R. (1984). Solute acquisition in glacial meltwaters, II Glacier d'Argentiere (French Alps): bulk meltwaters with open system characteristics. *Journal of Glaciology*, 30(104),44-48. https://doi.org/ 10.3189/S0022143000008479

Thomas, J., Joseph, S., & Thrivikramji, K. P. (2015). Hydro-chemical variations of a tropical mountain river system in a rain shadow region of the southern Western Ghats, Kerala, India. *Applied Geochemistry*, 63, 456-471. https://doi.org/10.1016/j.apgeochem.2015.03.018

Tiwari, S., Kumar, A., Gupta, A. K., Verma, A., Bhambri, R., Sundriyal, S., & Yadav, J. (2018). Hydrochemistry of meltwater draining from Dokriani Glacier during early and late ablation season, West Central Himalaya. *Himalayan Geology*, 39(1), 121-132.

Tranter, M., Sharp, M., Brown, G. H., Willis, I. C., Hubbard, B. P., Nielsen, M. K., ... Lamb, H. R. (1997). Variability in the chemical composition of in-situ subglacial meltwaters. *Hydrological Processess*, 11, 59-77. https://doi.org/10.1002/(SICI)1099-1085

Tranter, M., Brown, G. H., Raiswell, R., Sharp, M. J., & Gurnell, A. M. (1993). A conceptual model of solute acquisition by Alpine glacier meltwaters. *Journal of Glaciology*, 39(133), 573-581. https://doi.org/10.3189/S0022143000016464

Valder, J. F., Long, A. J., Davis, A. D., & Kenner, S. J. (2012). Multivariate statistical approach to estimate mixing proportions for unknown end members. *Journal of Hydrology*, 460, 65-76. https://doi.org/10.1016/j.jhydrol.2012.06.037

Wadham, J. L., Hodson, A. J., Tranter, M., & Dowdeswell, J. A. (1998). The hydrochemistry of meltwater draining a polythermal-based, high Arctic glacier, south Svalbard. *Hydrological Processes*, 12,1825-1849. https://doi.org/10.1002/(SICI)1099-1085(19981015)12:12<1825::AID-HYP669>3.0.CO;2-R

Xu, H., Hou, Z., An, Z., Liu, X., & Dong, J. (2010). Major ion chemistry of waters in Lake Qinghai catchments, NE Qinghai-Tibet plateau, China. *Quaternary International*, 212, 35-43. https://doi.org/10.1016/j.quaint.2008.11.001

Data Availability Statement

Due to the nature of this research, participants of this study did not agree for their data to be shared publicly, so supporting data is not available. However, the intermediate results supporting the findings of this study are available from the corresponding author upon reasonable request.

Captions of the figures

Figure 1 Location map of the study area.

Figure 2 (a). Snout of the Chaturangi glacier. (b). Longitudinal and transverse crevasses on the surface of the glacier. (c). A supraglacial lake on the surface of the glacier. (d). Discharge measurement and water sampling site near the snout of the glacier.

Figure 3 A simplified geological map of the upper reaches of Bhagirathi basin surrounding the glaciers (adapted from Searle et al. 1999).

Figure 4 Microphotographs of the rocks exposed along the catchment of Chaturangi glacier. (a). Harsil metasediment consisting of quartz, alkali feldspar, plagioclase feldspar, biotite and staurolite. (b). Martoli

formation metasediments consisting of quartz, alkali feldspar, plagioclase feldspar, biotite and garnet. (c). Biotite granite consisting of quartz, alkali feldspar, plagioclase feldspar and biotite. (d). Tourmaline granite consisting of quartz, alkali feldspar, plagioclase feldspar and tourmaline. Bt- biotite; Grt- garnet; Kfs- alkali feldspar; Pl-plagioclase feldspar; Qtz- quartz; St- staurolite; Tur- tourmaline.

Figure 5 Scatter plot between total cations and (Ca+Mg) for Chaturangi glacier meltwater to determining the weathering processes in the study area.

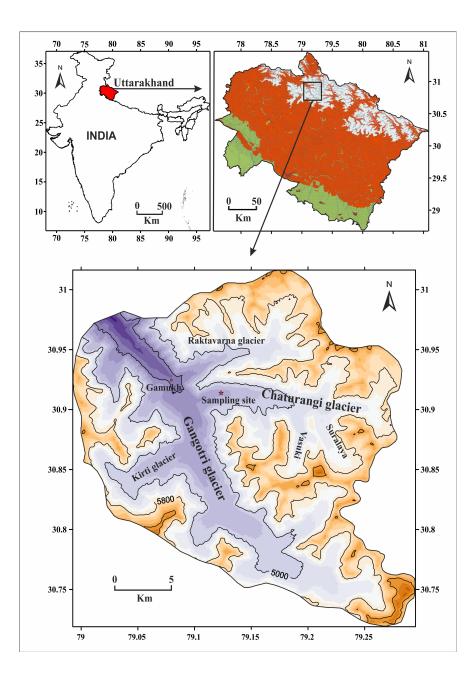
Figure 6 Scatter plot between total cations and (Na+K) for Chaturangi glacier meltwater to determining the weathering processes in the study area.

Figure 7 Scatter plot between (Ca+Mg) and SO_4 to determine the supply of sulphate in the meltwater.

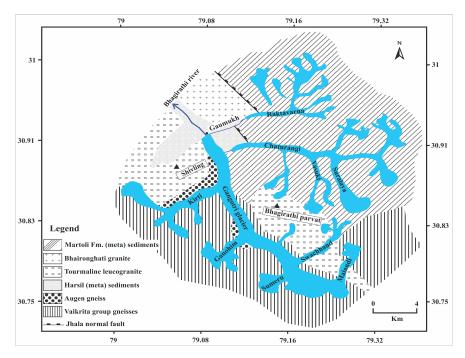
Figure 8 Scatter plot between (Na+K) and Cl to determine the contribution of ions in the meltwater from atmospheric input and other sources.

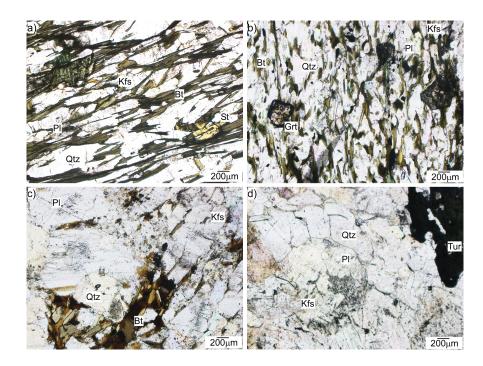
Figure 9 Piper plot for major ionic concentration to determine the chemical characterization and hydrogeochemical facies of meltwater.

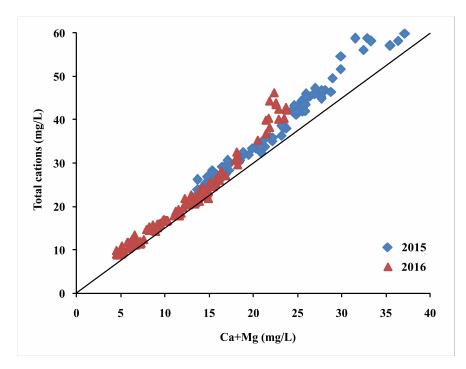
Figure 10 Gibbs plots between TDS vs Na/(Na+Ca) and TDS vs $Cl/(Cl+HCO_3)$ showing weathering of rocks mainly control the solute concentration in the meltwater followed by precipitation.

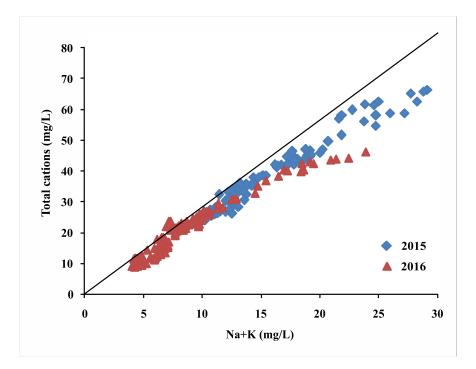


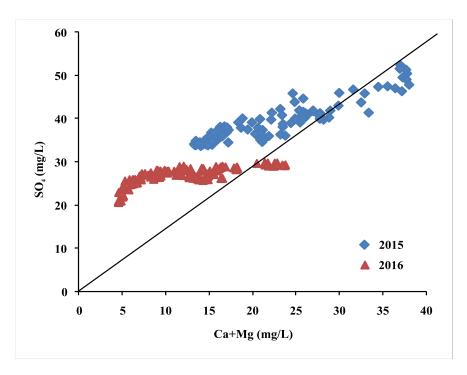


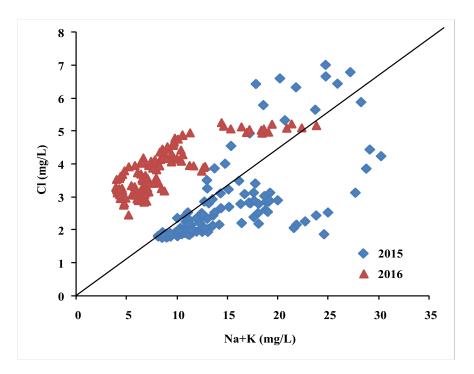


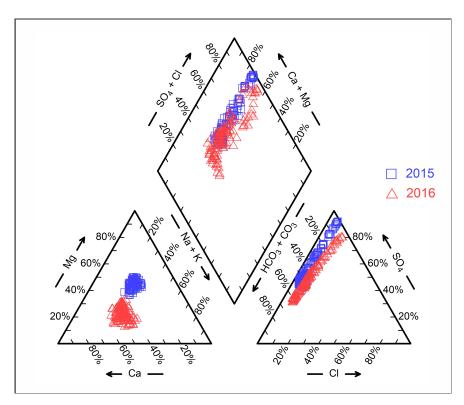




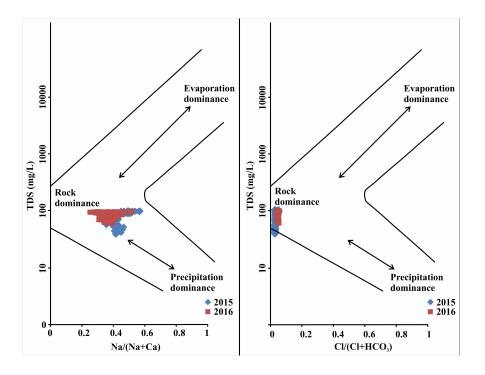








relimin	
el	
pr	
e.	
2	
ay	
В	
ta	
a d	
ġ.	
Ne.	
le	
revi	
Ser	
ğ	
B	
ě	
Ξ.	
not	
as 1	
ha	
-	
an	
nt	
preprint	
Id	
1.e	
This a	
H	
22	
10	
02	
663	
.6299(
98	
52	
36	
29	
2.1	
a.	
=	
10	
225	
10.22	
DI'G	
0	
0	
https://	
- https	
ht	
ission.	
-10	
18.	
Ξ.	
erm	
pe	
0	
hout pe	
hout pe	
without pe	
without pe	
without pe	
reuse without pe	
reuse without pe	
. No reuse without pe	
. No reuse without pe	
ed. No reuse without pe	
ed. No reuse without pe	
reserved. No reuse without pe	
ts reserved. No reuse without pe	
ghts reserved. No reuse without pe	
rights reserved. No reuse without pe	
rights reserved. No reuse without pe	
All rights reserved. No reuse without pe	
All rights reserved. No reuse without pe	
ider. All rights reserved. No reuse without pe	
All rights reserved. No reuse without pe	
/funder. All rights reserved. No reuse without pe	
ider. All rights reserved. No reuse without pe	
/funder. All rights reserved. No reuse without pe	
/funder. All rights reserved. No reuse without pe	
/funder. All rights reserved. No reuse without pe	
/funder. All rights reserved. No reuse without pe	
/funder. All rights reserved. No reuse without pe	
the author/funder. All rights reserved. No reuse without pe	
is the author/funder. All rights reserved. No reuse without pe	
is the author/funder. All rights reserved. No reuse without pe	
is the author/funder. All rights reserved. No reuse without pe	
is the author/funder. All rights reserved. No reuse without pe	
is the author/funder. All rights reserved. No reuse without pe	
ght holder is the author/funder. All rights reserved. No reuse without pe	
ght holder is the author/funder. All rights reserved. No reuse without pe	
copyright holder is the author/funder. All rights reserved. No reuse without pe	
copyright holder is the author/funder. All rights reserved. No reuse without pe	
The copyright holder is the author/funder. All rights reserved. No reuse without pe	
copyright holder is the author/funder. All rights reserved. No reuse without pe	
) — The copyright holder is the author/funder. All rights reserved. No reuse without pe	
) — The copyright holder is the author/funder. All rights reserved. No reuse without pe	
) — The copyright holder is the author/funder. All rights reserved. No reuse without pe	
) — The copyright holder is the author/funder. All rights reserved. No reuse without pe	
) — The copyright holder is the author/funder. All rights reserved. No reuse without pe	
) — The copyright holder is the author/funder. All rights reserved. No reuse without pe	
) — The copyright holder is the author/funder. All rights reserved. No reuse without pe	
) — The copyright holder is the author/funder. All rights reserved. No reuse without pe	
norea 11 Sep $2020 - $ The copyright holder is the author/funder. All rights reserved. No reuse without pe	
orea 11 Sep 2020 — The copyright holder is the author/funder. All rights reserved. No reuse without pe	
norea 11 Sep $2020 - $ The copyright holder is the author/funder. All rights reserved. No reuse without pe	
norea 11 Sep $2020 - $ The copyright holder is the author/funder. All rights reserved. No reuse without pe	
norea 11 Sep $2020 - $ The copyright holder is the author/funder. All rights reserved. No reuse without pe	
norea 11 Sep $2020 - $ The copyright holder is the author/funder. All rights reserved. No reuse without pe	
norea 11 Sep $2020 - $ The copyright holder is the author/funder. All rights reserved. No reuse without pe	



Hosted file

Table 1.docx available at https://authorea.com/users/356360/articles/479251-hydrogeochemicalanalysis-and-identification-of-weathering-processes-to-determine-the-solute-sources-inmeltwater-of-chaturangi-glacier-garhwal-himalaya-india

Hosted file

Table 2.docx available at https://authorea.com/users/356360/articles/479251-hydrogeochemicalanalysis-and-identification-of-weathering-processes-to-determine-the-solute-sources-inmeltwater-of-chaturangi-glacier-garhwal-himalaya-india

Hosted file

Table 3.docx available at https://authorea.com/users/356360/articles/479251-hydrogeochemicalanalysis-and-identification-of-weathering-processes-to-determine-the-solute-sources-inmeltwater-of-chaturangi-glacier-garhwal-himalaya-india

Hosted file

Table 4.docx available at https://authorea.com/users/356360/articles/479251-hydrogeochemicalanalysis-and-identification-of-weathering-processes-to-determine-the-solute-sources-inmeltwater-of-chaturangi-glacier-garhwal-himalaya-india

Hosted file

Table 5.docx available at https://authorea.com/users/356360/articles/479251-hydrogeochemicalanalysis-and-identification-of-weathering-processes-to-determine-the-solute-sources-inmeltwater-of-chaturangi-glacier-garhwal-himalaya-india